ATR disruption leads to chromosomal fragmentation and early embryonic lethality

Eric J. Brown and David Baltimore[1]

California Institute of Technology, Division of Biology, Pasadena, California 91125 USA

Although a small decrease in survival and increase in tumor incidence was observed in $ATR^{+/-}$ mice, $ATR^{-/-}$ embryos die early in development, subsequent to the blastocyst stage and prior to 7.5 days p.c. In culture, $ATR^{-/-}$ blastocysts cells continue to cycle into mitosis for 2 days but subsequently fail to expand and die of caspase-dependent apoptosis. Importantly, caspase-independent chromosome breaks are observed in $ATR^{-/-}$ cells prior to widespread apoptosis, implying that apoptosis is caused by a loss of genomic integrity. These data show that ATR is essential for early embryonic development and must function in processes other than regulation of p53.

ATM and ATR are mammalian counterparts to a family of high molecular weight protein kinases conserved in a broad range of species including *Schizosaccharomyces pombe*, *Saccharomyces cerevisiae*, and *Drosophila melanogaster* (Keith and Schreiber 1995; Keegan et al. 1996; Cimprich et al. 1996; Canman et al. 1998). The genes most closely related to *ATM* and *ATR* are the *MEC1* (*S. cerevisiae*) *TEL1* (*S. cerevisiae*), *RAD3* (*S. pombe*), and *Mei-41* (*D. melanogaster*) genes. Each of these genes is involved in DNA damage responses and falls into two groups based both on homology and function. *ATM* is related most closely to *TEL1*, a gene that shares an overlapping role with *MEC1* in checkpoint responses to γ-irradiation in *S. cerevisiae* (Morrow et al. 1995). *ATR*, on the other hand, is most closely related to *RAD3*, *Mei-41*, and *MEC1* in descending order of similarity. The kinase domain of *ATR* is 61% and 53% identical to the kinase domains of *RAD3* and *Mei-41*, respectively (Keith and Schreiber 1995; Cimprich et al. 1996; Keegan et al. 1996), whereas the *ATM* kinase domain shares only 39% identity with either *RAD3* or *Mei-41*.

Recent studies indicate that *ATR* functions in DNA damage response pathways similar to those mediated by RAD3, Mei-41, and MEC1. *RAD3*, *Mei-41*, and *MEC1* are required for checkpoint responses to pyrimidine dimer formation (UV radiation), DNA-alkylation (MMS), depletion of deoxyribonucleotides [hydroxyurea (HU)] and γ-irradiation (Weinert et al. 1994; Hari et al. 1995; Bentley et al. 1996). In addition to cell cycle checkpoint response, these genes have been implicated in the regulation of DNA repair (Weinert 1998). Consistent with the hypothesis that *ATR* is the functional mammalian homolog of *RAD3*, *Mei-41*, and *MEC1*, expression of a kinase inactive mutant of *ATR* (ATR–KI) sensitizes mammalian cells to these same forms of DNA damage and diminishes the G_2/M checkpoint response induced by γ-irradiation (Cliby et al. 1998; Wright et al. 1998). Recently, this ATR–KI cell line has been shown to be deficient in the regulated phosphorylation of p53 in response to UV and γ-irradiation (Tibbetts et al. 1999). Because *ATM*-disrupted cells are deficient in regulating p53 levels in response to γ-irradiation but not in response to UV or MMS (Canman et al. 1994; Xu and Baltimore 1996), ATR and ATM may possess both overlapping and nonredundant roles in regulating p53 (Canman et al. 1998; Tibbetts et al. 1999).

Here, we describe the phenotype of mice deficient in *ATR*. Whereas $ATR^{+/-}$ mice display a small decrease in survival and increase in tumor incidence, $ATR^{-/-}$ embryos die early in development. Early embryonic lethality and observations of $ATR^{-/-}$ blastocysts cultured in vitro indicate that *ATR* has an essential role in the proliferation of early embryonic cells. In addition, we show that $ATR^{-/-}$ cultured blastocyst cells suffer chromosomal fragmentation, suggesting that that the early death of $ATR^{-/-}$ embryos is caused by a widespread loss of genomic integrity. Because $ATM^{-/-}$ and $p53^{-/-}$ mice do not display a similar phenotype, these data indicate that ATR must function in some manner that is not redundant with *ATM* and is independent of p53 regulation. Evidence in support of a role for ATR in regulation of the *BRCA* gene products and in S- to M-phase transition of early embryonic cells is discussed.

Results

ATR *disruption*

Targeted disruption of *ATR* was achieved by deletion of three exons encoding the translation initiating methionine and the following 90 amino acids (Fig. 1A). Homologous recombination of the targeting vector into the *ATR* gene introduces a neomycin resistance cassette containing a single *Eco*RV site (Fig. 1A). This *Eco*RV site was subsequently used for colony screening by Southern blot (Fig. 1B) and the genotype of positive clones was confirmed further by PCR (Fig. 1C). Chimeric mice originating from three different ES cell clones transmitted the *ATR* disruption to F_1 offspring. Although quantitation of *ATR* mRNA in homozygous *ATR*-disrupted cells was not possible due to early embryonic lethality (below), ES cells and murine embryonic fibroblasts (MEFs) with a single *ATR* allele disrupted expressed 47% ± 7% (95% confidence interval) and 46% ± 10% less *ATR* mRNA, respectively (Fig. 1D). Truncated mRNA species in $ATR^{+/-}$ cells were not observed (Fig. 1D). Preliminary

[1]Corresponding author.
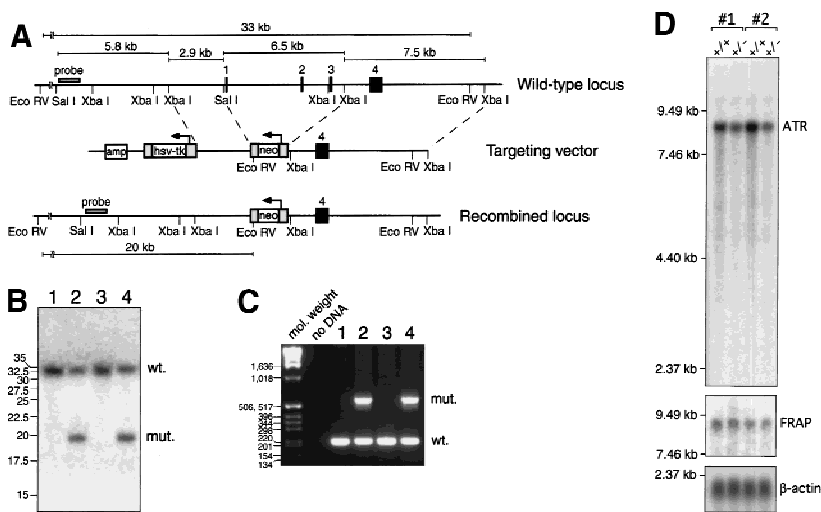E-MAIL baltimo@caltech.edu; FAX (626) 585-9495.

Figure 1. Targeted disruption of *ATR*. (*A*) A schematic of the wild-type locus, targeting vector, and recombined locus are shown. In the targeting vector and recombined locus, the neomycin selection cassette replaces the first three coding exons of *ATR*, including the translation initiation codon (exon 1). Homologous recombination of the targeting vector into the *ATR* locus introduces an *Eco*RV site, shortening a 33-kb wild-type *Eco*RV fragment to 20 kb. (*B*) Southern blot of DNA from ES cell colonies confirms the projected truncation of the *Eco*RV fragment by homologous recombination. (Lanes *1,3*) *Eco*RV-digested DNA from wild-type ES cells, (lanes *2,4*) ES cells with a single recombined *ATR* allele. (*C*) DNA samples from wild-type (lanes *1,3*) and *ATR*$^{+/-}$ (lanes *2,4*) ES cells were subjected to PCR to confirm genotyping as performed by Southern analysis. PCR products derived from wild-type and disrupted alleles are 216 and 590 bp, respectively. (*D*) Northern blot of poly (A)$^+$ mRNA from *ATR*$^{+/+}$ and *ATR*$^{+/-}$ MEFs. Embryos used to generate MEFs (passage 2) were isolated from *ATR*-disrupted mouse lines 1 and 2 (see Materials and Methods). Autoradiographic detection of *ATR*, *FRAP*, and β-*actin* transcripts are shown.

analysis of the effects of MMS, cisplatin, γ-irradiation, and HU on heterozygous ES cells and MEFs showed no significant differences in the survival of *ATR*$^{+/+}$ and *ATR*$^{+/-}$ cells (data not shown).

Increase in tumor incidence in ATR$^{+/-}$ mice

Although *p53*$^{+/-}$ mice exhibit decreased longevity and increased tumor incidence (Jacks et al. 1994), *ATM*$^{+/-}$ mice survive similarly to wild-type mice (Barlow et al. 1999; C. Barlow, pers. comm.). Because *ATR* and *ATM* are speculated to have both overlapping and nonredundant roles in regulating p53, we asked whether the longevity of *ATR*$^{+/-}$ mice is compromised. *ATR*$^{+/-}$ and *ATM*$^{+/-}$ mice (Xu and Baltimore 1996) were crossed to produce populations of *ATR*$^{+/-}$, *ATR*$^{+/-}ATM$^{+/-}$, and *ATM*$^{+/-}$ mice. Although no difference was observed in the survival of *ATR*$^{+/-}$ mice in comparison to *ATR*$^{+/-}ATM$^{+/-}$ mice, a decrease in the survival of both *ATR*$^{+/-}$ and *ATR*$^{+/-}ATM$^{+/-}$ mice was observed in comparison to that of *ATM*$^{+/-}$ mice. By 18 months, 10 of 48 *ATR*$^{+/-}$ (21%) and 8 of 41 *ATR*$^{+/-}ATM$^{+/-}$ mice (20%) had died in comparison to 1 of 22 *ATM*$^{+/-}$ mice (4.5%). Of the 10 *ATR*$^{+/-}$ and *ATR*$^{+/-}ATM$^{+/-}$ mice autopsied postmortem, 6 had evident tumors. The types of tumors observed

were histiocytic sarcoma (one in *ATR*$^{+/-}$; two in *ATR*$^{+/-}ATM$^{+/-}$), large follicular center cell lymphoma (*ATR*$^{+/-}$), gastric adenoma (*ATR*$^{+/-}ATM$^{+/-}$), and sebaceous gland adenoma (*ATR*$^{+/-}$).

To further examine the tumor incidence in these mice, autopsies were performed on the remaining *ATR*$^{+/-}$, *ATR*$^{+/-}ATM$^{+/-}$, and *ATM*$^{+/-}$ mice at 79–89 weeks of age [mean age = 83 ± 3 (s.d.) weeks]. In comparison to *ATM*$^{+/-}$ mice, a 4- and 2.6-fold increase in tumor incidence was observed in *ATR*$^{+/-}$ and *ATR*$^{+/-}ATM$^{+/-}$ mice, respectively. In total, 5 of 25 *ATR*$^{+/-}$ mice (20%), 4 of 30 *ATR*$^{+/-}ATM$^{+/-}$ mice (13%), and 1 of 21 *ATM*$^{+/-}$ mice (4.8%) had obvious tumors ranging from 1 to 3 cm in diameter. Comparison of the tumor incidence in *ATM*$^{+/-}$ mice with that observed in *ATR*$^{+/-}$ mice and in *ATR*$^{+/-}$ and *ATR*$^{+/-}ATM$^{+/-}$ mice combined was significant to *P* values of 0.050 and 0.045, respectively. The types of tumors observed were plasma cell lymphoma (*ATM*$^{+/-}$), mixed follicular center cell lymphoma (two in *ATR*$^{+/-}$; two in *ATR*$^{+/-}ATM$^{+/-}$), hepatocellular adenoma (one in *ATR*$^{+/-}$; one in *ATR*$^{+/-}ATM$^{+/-}$), fibrous histiocytoma (*ATR*$^{+/-}$), ovarian cystadenoma (*ATR*$^{+/-}$), and ovarian fibroma (*ATR*$^{+/-}ATM$^{+/-}$). Although Southern blot analysis of DNA extracted from *ATR*$^{+/-}$ and *ATR*$^{+/-}ATM$^{+/-}$ tumors did not indicate a loss of heterozygosity at the targeted region of *ATR* (data not shown), it is possible that alterations outside the targeted region may have occurred in these tumors given the large size of the *ATR* genomic locus (>60 kb). Together, these results indicate that in contrast to heterozygosity of the *ATM* gene, *ATR* heterozygosity causes a small decrease in survival and increase in tumor incidence.

ATR is required for early embryonic cellular proliferation

To generate homozygous *ATR*-disrupted mice, *ATR*$^{+/-}$ mice were intercrossed. However, of 225 progeny analyzed, no homozygous *ATR*-disrupted pups were observed, implying that *ATR* is essential for embryonic development. The stage at which *ATR*$^{-/-}$ embryos arrest in development was then determined by isolation of embryos from time-mated heterozygous crosses (Table 1). Although an abnormally high number of decidua contained embryos in the final stages of resorbtion, no viable *ATR*$^{-/-}$ embryos were observed at day 7.5 postcoitum (p.c.) or beyond. (Table 1). The high number of resorbed embryos, however, suggested that *ATR*$^{-/-}$ embryos survive earlier stages of development and die following implantion. To test whether *ATR*$^{-/-}$ embryos survive to the blastocyst stage, embryos were isolated 3.5 days p.c. and

Table 1. *Genotypic ratios of embryos from* ATR *heterozygous intercrosses*

Days p.c.	Viable embryos (litters)	+/+	+/−	−/−	Resorbed	*P* values
10.5–14.5	23 (5)	9	14	0	N.D.	0.003
8.5–9.5	23 (4)	6	17	0	4	0.003
7.5	35 (5)	11	24	0	12	0.0003

P values were calculated by one tailed *z*-test. (N.D.) Not determined.

genotyped. Of 83 embryos genotyped, 20 were *ATR*$^{-/-}$. Thus, *ATR*$^{-/-}$ embryos successfully develop to the blastocysts stage but die subsequently, prior to E7.5.

To determine if the developmental defect in *ATR*$^{-/-}$ mice was due to an inability of cells to proliferate subsequent to the blastocyst stage, day 3.5 embryos were isolated from *ATR*$^{+/-}$ intercrosses and grown in culture for 6 days. After 1 day in culture, *ATR*$^{+/+}$, *ATR*$^{+/-}$, and *ATR*$^{-/-}$ blastocysts hatched from the zona pellucida and implanted onto the tissue culture plastic. At isolation and during the first 2 days in culture, the inner cell mass (ICM) of *ATR*$^{-/-}$ blastocysts was indistinguishable from that of *ATR*$^{+/+}$ and *ATR*$^{+/-}$ blastocysts. However, while the ICM cells of *ATR*$^{+/+}$ and *ATR*$^{+/-}$ embryos continued to expand throughout the 6-day culture period, *ATR*$^{-/-}$ ICM cells failed to expand subsequent to day 2 and invariably died by day 4 in culture (Fig. 2A). Only the nondividing trophoblastic giant cells (TGC) of *ATR*$^{-/-}$ embryos remained after 6 days in culture (Fig. 2A). Identical results were observed with *ATR*$^{-/-}$ blastocysts (*n* = 8) derived from an independent *ATR*-disrupted line (line 2, data not shown).

The timing and cause of *ATR*$^{-/-}$ ICM cell death was then explored by TUNEL staining of blastocysts placed in culture for 48 or 72 hr. TUNEL staining detects extensive DNA fragmentation that results from apoptotic cell death. Although few TUNEL-stained cells were observed in *ATR*$^{-/-}$ blastocysts cultured for 48 hr, widespread TUNEL staining was observed after 72 hr (Fig. 2B). A majority of the TUNEL-stained *ATR*$^{-/-}$ cells was confirmed to be due to apoptosis through the use of the caspase 3-inhibitor Z-DEVD-FMK (Longthorne and Williams 1997). Caspase-3 is a protease required for initiation of apoptotic chromosome fragmentation following exposure of ES cells and other cell types to a vast array of DNA-damaging agents (Woo et al. 1998). The potent inhibitor of caspase-3, Z-DEVD-FMK, has been shown to inhibit Fas-induced apoptosis in T cells (Longthorne and Williams 1997). As shown, preincubation of *ATR*$^{-/-}$ blastocyst cells with Z-DEVD-FMK inhibited the TUNEL staining observed after 48 and 72 hr of culture (Fig. 2B). Overall, the number of TUNEL-stained cells in *ATR*$^{-/-}$ blastocysts was reduced 80% by preincubation with Z-DEVD-FMK. Consistent with caspase-3 knockout studies (Woo et al. 1998), Z-

DEVD-FMK did not rescue *ATR*$^{-/-}$ cells from other morphological effects of apoptosis such as changes in nuclear morphology (Fig. 2B, day 3). These results demonstrate that *ATR* is essential for expansion of early embryonic cells in culture and that loss of *ATR* ultimately results in apoptotic cell death.

Chromosome fragmentation in ATR$^{-/-}$ cells

Given the potential role of ATR in DNA replication and damage checkpoints and DNA repair, we speculated that the apoptotic signal in *ATR*$^{-/-}$ ICM cells may be initiated by damaged DNA resulting from the lack of *ATR*. If so, one would expect that such damage would occur equally in the presence and absence of Z-DEVD-FMK. To examine this possibility, mitotic spreads were prepared from blastocysts grown for 48 hr in culture and then treated with nocodazole or left untreated for 6 hr. The number of mitotic cells in *ATR*$^{-/-}$ blastocyst cultures increased significantly upon treatment with nocodazole, indicating that *ATR*$^{-/-}$ cells attempt proliferation at day 2 in culture (Table 2). However, consistent with the hypothesis that disruption of *ATR* causes a loss of genomic
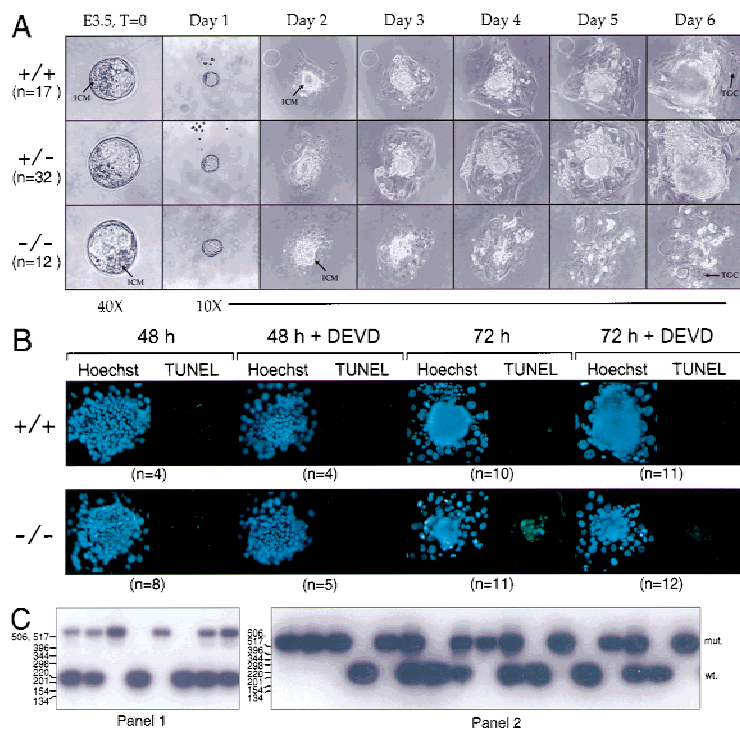

Figure 2. Deletion of *ATR* leads to apoptotic death of early embryonic cells. (*A*) Day 3.5 p.c. blastocysts were isolated from *ATR*$^{+/-}$ intercrosses and were cultured in 96-well plates for 6 days. ICMs and TGC are indicated. (*B*) TUNEL staining of *ATR*$^{+/-}$ and *ATR*$^{-/-}$ blastocysts cultured in the presence or absence of Z-DEVD-FMK. Blastocysts isolated from *ATR*$^{+/-}$ intercrosses were cultured in Terasaki-style microwell plates (Nunc) for 48 and 72 hr. Z-DEVD-FMK (200 μM) or vehicle was added after 24 hr of culture (for 48- and 72-hr time points) and added again after 48 hr (72-hr time point). Fluorescein (TUNEL) and Hoechst fluorescent images are shown. (*C*) Examples of PCR genotyping of blastocysts cultured as described in *A* and *B* are shown in panels *1* and *2*, respectively.

Table 2. *Mitotic index and analysis of mitotic spreads from blastocysts cultured for 2 days in vitro*

Genotype[a]	N[b]	DEVD	Total cells/ blastocyst[c]	Percent[c] mitotic	Percent[c] fragmented
+/+ (4)	−	−	164 ± 95	1 ± 1	0
+/+ (6)	+	−	111 ± 67	25 ± 10	0
+/+ (5)	+	+	100 ± 14	21 ± 8	0
+/− (7)	−	−	158 ± 57	1 ± 0.8	0
+/− (7)	+	−	115 ± 41	23 ± 11	2 ± 3
+/− (6)	+	+	142 ± 47	20 ± 8	0
−/− (7)	−	−	133 ± 41	3 ± 2	60 ± 45
−/− (7)	+	−	79 ± 24	12 ± 5	64 ± 22
−/− (6)	+	+	81 ± 47	13 ± 7	65 ± 21

[a]The number of blastocysts analyzed per condition are indicated in parentheses.
[b]Nocodazole.
[c]Confidence intervals (95%) are shown following the ± symbol.

integrity, chromosomal fragmentation was apparent in >60% of the mitotic spreads from $ATR^{-/-}$ cells and appeared equally with or without Z-DEVD-FMK pre-incubation (Table 2). Thus, the Z-DEVD-FMK-resistant chromosomal fragmentation observed in $ATR^{-/-}$ blastocysts at day 2 in culture (Fig. 3) correlates to and is the likely cause of the widespread caspase-dependent apoptosis observed at day 3 (Fig. 2B). As shown, chromosome fragmentation ranged from mild (Fig. 3A) to extensive (Fig. 3B). This extensive mitotic DNA fragmentation (Fig. 3B) may contribute to the residual caspase-independent TUNEL staining observed in the presence of Z-DEVD-FMK (discussed above); however, the degree of fragmen-
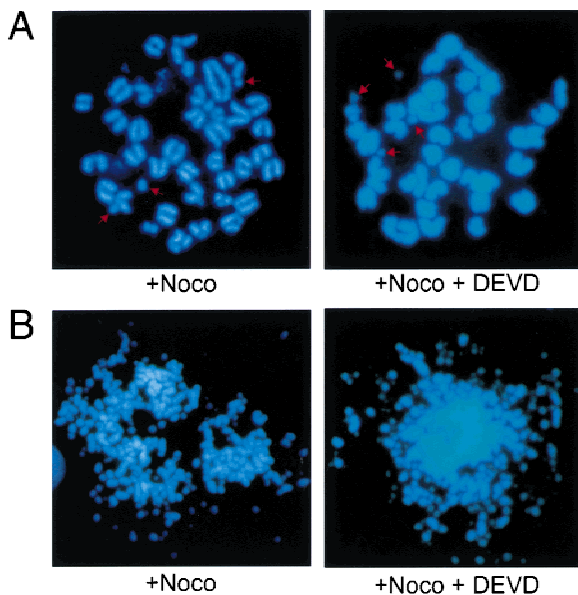

Figure 3. Chromosomal fragmentation in $ATR^{-/-}$ cells at day 2 in culture. Chromosome fragmentation was observed ranging from few (*A*) to many (*B*) breaks. This range of fragmentation was observed similarly in $ATR^{-/-}$ blastocysts cultured in the presence or absence of 200 μM Z-DEVD-FMK added after 24 hr of culture.

tation observed in a majority of mitotic spreads was apparently beyond the limits of detection by TUNEL. Although we cannot rule out the possibility that the observed chromosome fragmentation in $ATR^{-/-}$ cells may result from early stages of a caspase-independent apoptotic process, these data are consistent with the hypothesis that the aborted development of $ATR^{-/-}$ embryos results from a loss of genomic integrity.

Discussion

We have found that disruption of the *ATR* gene leads to a small increase in tumorigenesis in heterozygotes and very early embryonic lethality in homozygotes. Although the total incidence of tumors in *ATR* heterozygotes was not as great as those observed in *p53* heterozygotes (Jacks et al. 1994), the effect of *ATR* heterozygosity was statistically significant. It is interesting to note that the incidence of large benign tumors was particularly increased in *ATR* heterozygotes. This increase in benign tumors may indicate that deficiency in *ATR* has a greater effect on the rate of tumor initiation than on the rate of progression to malignancy. It is currently not known whether *ATR* defects exist in humans; however the region to which *ATR* maps in humans is a site of genetic alteration in lung cell carcinomas (Cimprich et al. 1996)

As described here, our data indicate that ATR has an essential role in preventing the occurrence of DNA damage early in embryogenesis. Although recent studies suggest that ATR regulates p53, defective regulation of p53 is unlikely to be the sole cause of such DNA damage, as $p53^{-/-}$ mice do not suffer a block in early embryonic development similar to that observed in $ATR^{-/-}$ mice. Based on previous studies and data provided in this paper, two plausible essential roles for ATR are apparent and are discussed here: regulation of the *BRCA* gene products and control of the S- to M-phase transition.

BRCA1 and BRCA2 regulation

Several lines of evidence have substantiated a link between ATR and the functions of BRCA1 and BRCA2. $BRCA1^{-/-}$, $BRCA2^{-/-}$, and $RAD51^{-/-}$ mice die early in development and have cellular proliferation defects similar to that observed in $ATR^{-/-}$ cultured blastocysts (Hakem et al. 1996; Lim and Hasty 1996; Sharan et al. 1997; Suzuki et al. 1997). Secondly, like $ATR^{-/-}$ cells, chromosome breaks are observed in $RAD51^{-/-}$, *BRCA1* exon 11-deleted, and *BRCA2*-truncated cells (Lim and Hasty 1996; Patel et al. 1998; Xu et al. 1999). Finally, the *ATR* homolog *ATM* recently has been shown to be required for the phosphorylation of BRCA1 in response to γ-irradiation but is dispensable for BRCA1 phosphorylation in response to HU, MMS, and UV (Scully et al. 1997; Cortez et al. 1999). Because ATR–KI expression renders cells sensitive to these later reagents (Cliby et al. 1998; Wright et al. 1998), it is possible that ATR and ATM both regulate BRCA1 phosphorylation, albeit in a DNA damage-specific manner. These genetics and biochemical similarities provide correlative evidence that the

BRCA gene products may be dependent on ATR function.

S- to M-phase transition

A second plausible essential function for ATR is suggested by the similarity between the extensive chromosomal fragmentation in $ATR^{-/-}$ cells (Fig. 3B) and that observed in cells undergoing mitotic catastrophe. Mitotic catastrophe is caused by premature entry of cells into mitosis prior to completion of DNA synthesis and is characterized by a high degree of chromosomal fragmentation (Heald et al. 1993; Schlegel and Pardee 1986). The treatments and mutations that cause mitotic catastrophe are now recognized to influence a pathway that regulates DNA damage and replication checkpoints in mammalian cells and *S. pombe* (Heald et al. 1993; Russell 1998; Chan et al. 1999; Pines 1999). Importantly, in *S. pombe* this pathway requires *RAD3*, the closest known relative of *ATR* (Cimprich et al. 1996; Keegan et al. 1996). Although recent studies indicate ATR may have a redundant role with ATM in regulating this checkpoint pathway in response to γ-irradiation (Cliby et al. 1998; Matsuoka et al. 1998; Chaturvedi et al. 1999), an essential role for ATR in DNA replication checkpoint responses has been implied (Cliby et al. 1998; Chaturvedi et al. 1999; Sarkaria et al. 1999).

If ATR regulates a DNA replication checkpoint in mammalian cells, mitotic catastrophe in $ATR^{-/-}$ cells might be due to the lack of such a checkpoint combined with the extremely rapid cellular proliferation that occurs normally in the course of early embryonic development. Early embryonic cells proliferate with doubling times as short as 2 hr at day 6.5 p.c. (Snow 1977) and can completely lack a G_2 phase (Aladjem et al. 1998). Such rapid proliferation indicates a high degree of precision in transition from S to M phase. Thus, the chromosomal fragmentation in $ATR^{-/-}$ cells might be due to an inability to coordinate this transition accurately, resulting in premature entry into mitosis. According to this analysis, ATR may be dispensable in cells that cycle through a more extensive G_2 phase, but might be particularly essential in the early embryo to sense incomplete DNA replication and prevent mitotic catastrophe.

Materials and methods

Generation of the ATR targeted allele
A 17-kb genomic fragment encoding the amino terminus of murine *ATR* was cloned from a 129SVJ genomic library (Stratagene). The *ATR* targeting vector was constructed by subcloning the 2.9-kb *Sal*I and 7.5-kb *Xba*I genomic fragments flanking the 6.5-kb *ATR* amino terminal encoding fragment into the pPNT vector (Fig. 1A). *ATR*-disrupted ES cells cells were generated in both D3 and J1 lines. A single targeted allele was observed in 9 of 310 isolated ES cell colonies. Isolated colonies were expanded and DNA was prepared by digestion in PK buffer (100 mM Tris at pH 8.0, 400 mM NaCl, 5 mM EDTA, 0.8% SDS), followed by extraction with one-third volume of saturated NaCl and precipitation in an equal volume of isopropanol. *Eco*RV fragments were separated on a 0.66% agarose gel and detected by Southern analysis using the indicated probe (Fig. 1A). *ATR*-disrupted lines 1 and 2 are derived from J1 and D3 ES cell lines, respectively. PCR genotyping was performed using a common primer, 121 bp 5′ of the initiating methionyl codon in exon 1 (5′-ttccgg-gaggagaattttggac-3′) in combination with primers discriminating wild-

type exon 1-containing alleles (5′-cggcgactcgaagctggcgacgacgc-3′) and knockout alleles encoding the 3′ end of the neomycin resistance gene (5′-cagcgcatcgccttctatcgccttcttgac-3′). PCR was performed in 25-µl reactions with 1× PCR buffer (Boehringer Mannheim), 1.25 units of *Taq* polymerase, and 2% DMSO. Temperature cycling conditions were (1) 94°C for 4 min, (2) 94°C for 1 min, (3) 62°C for 2.5 min, and (4) 72°C for 2.5 min, cycling 33 times to step 2. Poly (A)+ mRNA from ES cells and day 14.5 MEFs was isolated, subjected to Northern blot analysis, and probed with the full-length human *ATR* cDNA (Cimprich et al. 1996). Normalization was performed upon subsequent probing with the full-length cDNAs for *FRAP* (Brown et al. 1994) and *β-actin* (Clontech). Levels of mRNA were quantitated by PhosphorImager readout (Molecular Dynamics), and 95% confidence intervals for the average reduction of normalized *ATR* mRNA levels were calculated by Student's *t*-test.

Survival of and tumors in ATR+/− mice
$ATR^{+/-}$ and $ATM^{+/-}$ of 129Sv and C57BL/6 mixed background were intercrossed to produce populations of $ATR^{+/-}$, $ATR^{+/-}ATM^{+/-}$, and $ATM^{+/-}$ mice. Mice suffering from severe fighting wounds (~10%) were excluded from further study. The percentages of deceased and euthanized mice from $ATR^{+/-}$ and $ATR^{+/-}ATM^{+/-}$ populations were compared to that of $ATM^{+/-}$ by Kaplan–Meier analysis, and log-rank *P* values were calculated (Biostat 2000, Cupertino, CA). Individual comparison of $ATR^{+/-}$ and $ATR^{+/-}ATM^{+/-}$ survival with $ATM^{+/-}$ survival was significant to *P* values of 0.067 and 0.097, respectively. Histopathology on formalin-fixed tissues was performed by the Research Animal Diagnostic and Investigative Laboratory (Columbia, MO). Test significance of difference in tumor incidence for animals autopsied 79–89 weeks of age was calculated by one tailed *z*-test.

Cultured blastocysts and TUNEL assays
Blastocysts were flushed from the uterus of $ATR^{+/-}$ females 3.5 days p.c. and washed five times in M2 media (Sigma) or PBS containing 5% FBS. Blastocysts were cultured for the times indicated in 50 µl (Fig. 2A) or 15 µl (Fig. 2B) of DMEM containing 15% FBS, 100 µM β-mercaptoethanol, 2 mM glutamine, 100 µM nonessential amino acids, and 1× penicillin/streptomycin (GIBCO–BRL). Z-DEVD-FMK (200 µM) or vehicle was added after 24 and 48 hr (72-hr time point) of culture. At 200 µM, Z-DEVD-FMK has been shown to completely prevent Fas-induced apoptosis in human cells without affecting cellular proliferation (Longthorne and Williams 1997). For TUNEL assay, blastocysts were fixed at the indicated times in 3% paraformaldhyde/PBS for 30 min. Permeabilization and TUNEL assays were performed using the In Situ Cell Death Detection Kit, Fluorescein (Boehringer Mannheim) as per the manufacturer's instructions. For PCR genotyping, DNA was prepared by incubation of individual blastocysts with 1.5 µl of NSPK buffer [300 µg/ml proteinase K (Boehringer Mannheim), 100 mM KCl, 20 mM Tris at pH 8.0, 4 mM MgCl₂, 0.9% NP-40, 0.9% Triton X-100] for 4 hr at 60°C, followed by incubation at 90°C for 30 min. The entire DNA isolate was used directly for PCR, which was performed as described for Figure 1C. PCR products were then Southern blotted and probed with a ³²P end-labeled internal primer common to both wild-type and mutant PCR products (5′-gacctcgcggggctcc-gtcga-3′). Hybridized products were detected by autoradiography.

Preparation of mitotic spreads and genotyping
Blastocysts were grown in 96-well round-bottom plates as described (Fig. 2A) and treated with 200 µM Z-DEVD-FMK or vehicle (0.1% DMSO) after 24 and 48 hr in culture. At 48 hr in culture, blastocysts were treated with 2.5 µM nocodazole for 6 hr and subsequently processed for preparation of mitotic spreads. To suspend cells, blastocysts were washed twice in PBS and trypsinized in 30 µl of 0.25% trypsin/1 mM EDTA (GIBCO–BRL). Trypsin was then neutralized with 150 µl of culture media and, cells were tritiated and transferred to 200-µl micocentrifuge tubes. At this step, 60 µl of the cell suspension was transferred to a separate tube for PCR analysis (below). The remaining 120-µl cell suspension was washed once in PBS (250 g centrifugation), resuspended in 75 mM KCl, and incubated at room temperature for 20 min. Cells were then centrifuged at 500*g*, resuspended in ice-cold 3:1 (vol/vol) methanol/acetic acid fixative, incubated at 4°C for 10 min, and centrifuged at 650*g*. The fixation steps were repeated once, and cells were resuspended in 15 µl of fixative and dropped onto prewarmed (37°C) glass slides. Slides were stained with Hoechst or Giemsa, and mitotic and interphase cells were counted. Confidence intervals (95%) were calculated by Student's *t*-test. For genotyp-

ing, cells (60 µl, above) were washed five times with PBS (250g centrifugation). All centrifugation steps in these procedures were for 5 min. The final cell pellet was resupended in 1.5 µl of NSPK buffer, and DNA was isolated and PCR genotyped as described above.

Acknowledgments

References

Aladjem, M.I., B.T. Spike, L.W. Rodewald, T.J. Hope, M. Klemm, R. Jaenisch, and G.M. Wahl. 1998. ES cells do not activate p53-dependent stress responses and undergo p53- independent apoptosis in response to DNA damage. *Curr. Biol.* **8:** 145–155.

Barlow, C., M.A. Eckhaus, A.A. Schaffer, and A. Wynshaw-Boris. 1999. Atm haploinsufficiency results in increased sensitivity to sublethal doses of ionizing radiation in mice. *Nat. Genet.* **21:** 359–360.

Bentley, N.J., D.A. Holtzman, G. Flaggs, K.S. Keegan, A. DeMaggio, J.C. Ford, M. Hoekstra, and A.M. Carr. 1996. The Schizosaccharomyces pombe rad3 checkpoint gene. *EMBO J.* **15:** 6641–6651.

Brown, E.J., M.W. Albers, T.B. Shin, K. Ichikawa, C.T. Keith, W.S. Lane, and S.L. Schreiber. 1994. A mammalian protein targeted by G1-arresting rapamycin-receptor complex. *Nature* **369:** 756–758.

Canman, C.E., A.C. Wolff, C.Y. Chen, A.J. Fornace, Jr., and M.B. Kastan. 1994. The p53-dependent G1 cell cycle checkpoint pathway and ataxia-telangiectasia. *Cancer Res.* **54:** 5054–5058.

Canman, C. E., D.S. Lim, K.A. Cimprich, Y. Taya, K. Tamai, K. Sakaguchi, E. Appella, M.B. Kastan, and J.D. Siliciano. 1998. Activation of the ATM kinase by ionizing radiation and phosphorylation of p53. *Science* **281:** 1677–1679.

Chan, T.A., H. Hermeking, C. Lengauer, K.W. Kinzler and B. Vogelstein. 1999. 14-3-3 Sigma is required to prevent mitotic catastrophe after DNA damage. *Nature* **401:** 616–620.

Chaturvedi, P., W.K. Eng, Y. Zhu, M.R. Mattern, R. Mishra, M.R. Hurle, X. Zhang, R.S. Annan, Q. Lu, L.F. Faucette et al. 1999. Mammalian Chk2 is a downstream effector of the ATM-dependent DNA damage checkpoint pathway. *Oncogene* **18:** 4047–4054.

Cimprich, K.A., T.B. Shin, C.T. Keith, and S.L. Schreiber. 1996. cDNA cloning and gene mapping of a candidate human cell cycle checkpoint protein. *Proc. Natl. Acad. Sci.* **93:** 2850–2855.

Cliby, W.A., C.J. Roberts, K.A. Cimprich, C.M. Stringer, J.R. Lamb, S.L. Schreiber, and S.H. Friend. 1998. Overexpression of a kinase-inactive ATR protein causes sensitivity to DNA-damaging agents and defects in cell cycle checkpoints. *EMBO J.* **17:** 159–169.

Cortez, D., Y. Wang, J. Qin, and S.J. Elledge. 1999. Requirement of ATM-dependent phosphorylation of Brca1 in the DNA damage response to double-strand breaks. *Science* **286:** 1162–1166.

Hakem, R., J.L. de la Pompa, C. Sirard, R. Mo, M. Woo, A. Hakem, A. Wakeham, J. Potter, A. Reitmair, F. Billia et al. 1996. The tumor suppressor gene Brca1 is required for embryonic cellular proliferation in the mouse. *Cell* **85:** 1009–1023.

Hari, K.L., A. Santerre, J.J. Sekelsky, K.S. McKim, J.B. Boyd, and R.S. Hawley. 1995. The mei-41 gene of D. melanogaster is a structural and functional homolog of the human ataxia telangiectasia gene. *Cell* **82:** 815–821.

Heald, R., M. McLoughlin, and F. McKeon. 1993. Human wee1 maintains mitotic timing by protecting the nucleus from cytoplasmically activated Cdc2 kinase. *Cell* **74:** 463–474.

Jacks, T., L. Remington, B.O.Williams, E.M. Schmitt, S. Halachmi, R.T.

Bornson, and R.A. Weinberg. 1994. Tumor spectrum analysis in p53-mutant mice. *Curr. Biol.* **4:** 1–7.

Keegan, K.S., D.A. Holtzman, A.W. Plug, E.R. Christenson, E.E. Brainerd, G. Flaggs, N.J. Bentley, E.M. Taylor, M.S. Meyn, S.B. Moss et al. 1996. The Atr and Atm protein kinases associate with different sites along meiotically pairing chromosomes. *Genes & Dev.* **10:** 2423–2437.

Keith, C.T. and S.L. Schreiber. 1995. PIK-related kinases: DNA repair, recombination, and cell cycle checkpoints. *Science* **270:** 50–51.

Lim, D.-S. and P. Hasty. 1996. A mutation in mouse rad51 results in an early embryonic lethal that is suppressed by a mutation in p53. *Mol. Cell. Biol.* **16:** 7133–7143.

Longthorne, V.L. and G.T. Williams. 1997. Caspase activity is required for commitment to Fas-mediated apoptosis. *EMBO J.* **16:** 3805–3812.

Matsuoka, S., M. Huang, and S. J. Elledge. 1998. Linkage of ATM to cell cycle regulation by the Chk2 protein kinase. *Science* **282:** 1893–1897.

Morrow, D.M., D.A. Tagle, Y. Shiloh, F.S. Collins, and P. Hieter. 1995. TEL1, an S. cerevisiae homolog of the human gene mutated in ataxia telangiectasia, is functionally related to the yeast checkpoint gene MEC1. *Cell* **82:** 831–840.

Patel, K.J., V.P. Vu, H. Lee, A. Corcoran, F.C. Thistlethwaite, M.J. Evans, W.H. Colledge, L.S. Friedman, B.A. Ponder, and A.R. Venkitaraman. 1998. Involvement of Brca2 in DNA repair. *Mol. Cell* **1:** 347–357.

Pines, J. 1999. Cell cycle. Checkpoint on the nuclear frontier. *Nature* **397:** 104–105.

Russell, P. 1998. Checkpoints on the road to mitosis. *Trends Biochem. Sci.* **23:** 399–402.

Sarkaria, J.N., E.C. Busby, R.S. Tibbetts, P. Roos, Y. Taya, L.M. Karnitz, and R.T. Abraham. 1999. Inhibition of ATM and ATR kinase activities by the radiosensitizing agent, caffeine. *Cancer Res.* **59:** 4375–4382.

Schlegel, R. and A.B. Pardee. 1986. Caffeine-induced uncoupling of mitosis from the completion of DNA replication in mammalian cells. *Science* **232:** 1264–1266.

Scully, R., J. Chen, R.L. Ochs, K. Keegan, M. Hoekstra, J. Feunteun, and D.M. Livingston. 1997. Dynamic changes of BRCA1 subnuclear location and phosphorylation state are initiated by DNA damage. *Cell* **90:** 425–435.

Sharan, S.K., M. Morimatsu, U. Albrecht, D.S. Lim, E. Regel, C. Dinh, A. Sands, G. Eichele, P. Hasty, and A. Bradley. 1997. Embryonic lethality and radiation hypersensitivity mediated by Rad51 in mice lacking Brca2. *Nature* **386:** 804–810.

Snow, M.H.L. 1977. Gastrulation in the mouse: Growth and regionalization of the epiblast. *J. Embryol. Exp. Morphol.* **42:** 293–303.

Suzuki, A., J.L. de la Pompa, R. Hakem, A. Elia, R. Yoshida, R. Mo, H. Nishina, T. Chuang, A. Wakeham, A. Itie et al. 1997. Brca2 is required for embryonic cellular proliferation in the mouse. *Genes & Dev.* **11:** 1242–1252.

Tibbetts, R.S., K.M. Brumbaugh, J.M. Williams, J.N. Sarkaria, W.A. Cliby, S.Y. Shieh, Y. Taya, C. Prives, and R.T. Abraham. 1999. A role for ATR in the DNA damage-induced phosphorylation of p53. *Genes & Dev.* **13:** 152–157.

Weinert, T. 1998. DNA damage and checkpoint pathways: Molecular anatomy and interactions with repair. *Cell* **94:** 555–558.

Weinert, T.A., G.L. Kiser, and L.H. Hartwell. 1994. Mitotic checkpoint genes in budding yeast and the dependence of mitosis on DNA replication and repair. *Genes & Dev.* **8:** 652–665.

Woo, M., R. Hakem, M.S. Soengas, G.S. Duncan, A. Shahinian, D. Kagi, A. Hakem, M. McCurrach, W. Khoo, S.A. Kaufman et al. 1998. Essential contribution of caspase 3/CPP32 to apoptosis and its associated nuclear changes. *Genes & Dev.* **12:** 806–819.

Wright, J.A., K.S. Keegan, D.R. Herendeen, N.J. Bentley, A.M. Carr, M.F. Hoekstra, and P. Concannon. 1998. Protein kinase mutants of human ATR increase sensitivity to UV and ionizing radiation and abrogate cell cycle checkpoint control. *Proc. Natl. Acad. Sci.* **95:** 7445–7450.

Xu, X., Z. Weaver, S.P. Linke, C. Li, J. Gotay, X.W. Wang, C.C. Harris, T. Ried, and C.X. Deng. 1999. Centrosome amplification and a defective G2-M cell cycle checkpoint induce genetic instability in BRCA1 exon 11 isoform-deficient cells. *Mol. Cell* **3:** 389–395.

Xu, Y. and D. Baltimore. 1996. Dual roles of ATM in the cellular response to radiation and in cell growth control. *Genes & Dev.* **10:** 2401–2410.